JACS
JOURNAL OF THE AMERICAN CHEMICAL SOCIETY

Article

pubs.acs.org/JACS

Zwitterions and Unobserved Intermediates in Organocatalytic Diels–Alder Reactions of Linear and Cross-Conjugated Trienamines

Arne Dieckmann,[‡] Martin Breugst,[‡] and K. N. Houk*

Department of Chemistry and Biochemistry, University of California—Los Angeles, 607 Charles E. Young Drive East, Los Angeles, California 90095-1569, United States

Supporting Information

ABSTRACT: The Diels–Alder reactions of cyclic linear and cross-conjugated trienamines with oxindoles have been studied with density functional theory [M06-2X/def2-TZVPP/IEFPCM//B97D/6-31+G(d,p)/IEFPCM]. These reactions are found to proceed in a stepwise fashion. Computations revealed that these transformations involve complex mechanisms including zwitterionic intermediates and several unstable alternate cycloadducts arising from (2 + 2) cycloadditions and hetero-Diels–Alder reactions. The observed regio- and stereochemistry can be rationalized by a combination of kinetic and thermodynamic control.

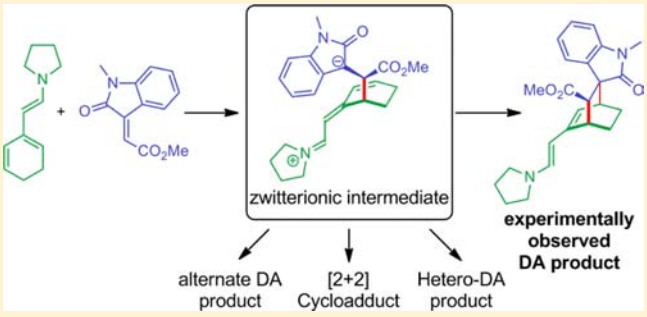

INTRODUCTION

The field of organocatalysis has enjoyed an impressive success over the past decade.[1] Within the framework of aminocatalysis, iminium,[1d] enamine,[1e] dienamine,[1i] and SOMO activation[1f] have been developed to become powerful synthetic tools. Organocatalytic cycloadditions and in particular Diels–Alder reactions have been studied in many contexts.[2] Frontier Molecular Orbital Theory predicts that raising the HOMO energy results in lower activation barriers,[3] explaining the excellent reactivities of enamines and dienamines reactants in such transformations.[4]

In 2011, Chen, Jørgensen, and co-workers extended the concept of dienamine catalysis[4e] to linear trienamine intermediates.[4j,k] Trienamines derived from secondary amines and dienals display high activities as dienes in Diels–Alder cycloaddition reactions. Excellent stereoselectivities were either achieved by steric effects or hydrogen bonding employing a squaramide-based catalyst.[5]

Recently, Jørgensen and co-workers reported on the [4 + 2] cycloadditions of cyclic cross-conjugated trienamines, a new concept in asymmetric organocatalysis.[6] Surprisingly, only products of the reaction of the cross-conjugated trienamine **3** derived from aldehyde **1** with the alkylidene oxindole **4** and no products of the linear trienamine isomer **2** were observed (Scheme 1). In order to explain the remarkable selectivity, the authors conducted a computational study based on a truncated model system employing density functional theory. Their gas-phase calculations at the MPW1K/6-31+G(d,p) level of theory suggested an asynchronous but concerted mechanism. Zwitterionic intermediates could not be located on this potential energy surface. The observation of **5** as the only product was explained by thermodynamic control.[6] However, the free energy barriers for the backward reactions were calculated to be >30 kcal mol^{-1}. These barriers make it unlikely that the kinetically favored product could undergo a retro-Diels–Alder reaction under the reaction conditions. As the trienamine **3** gives Michael adducts with vinyl bissulfones,[6] and dienamines undergo stepwise [2 + 2] cycloadditions with nitroolefins,[4n] it seemed likely that the cycloaddition reactions of **2** or **3** with **4** would occur in a stepwise manner.

Scheme 1. Experimentally Observed Regioselectivities in Diels-Alder-Reactions of Trienamines 2 and 3 and Oxindole 4 (from ref 6)

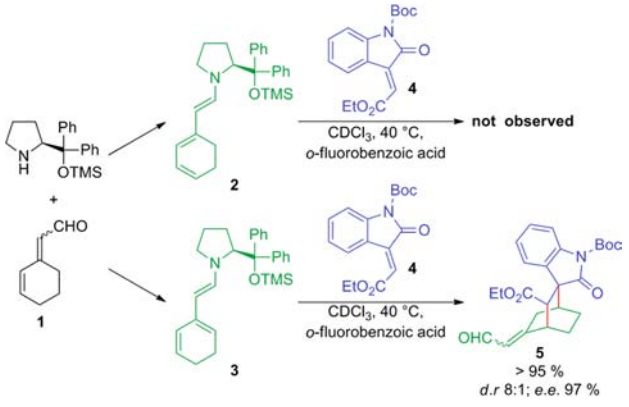

The design of new organocatalysts and transformations relies on a detailed understanding of the factors governing the stereo- and regiochemistry. In particular, knowledge about thermodynamic or kinetic control is highly important for rational design approaches. To elucidate alternative origins for the observed regio- and stereoselectivities, we undertook a thorough computational analysis, initially employing the same truncated

Received: December 10, 2012
Published: January 27, 2013

   dx.doi.org/10.1021/ja312043g | J. Am. Chem. Soc. 2013, 135, 3237–3242

Scheme 2. Reaction Pathways for Cycloadditions of Linear Trienamines 6 with the Oxindole 7 [Free Energies with Respect to 6 + 7, in kcal mol^{-1}; M06-2X/def2-TZVPP/IEFPCM//B97D/6-31+G(d,p)/IEFPCM]

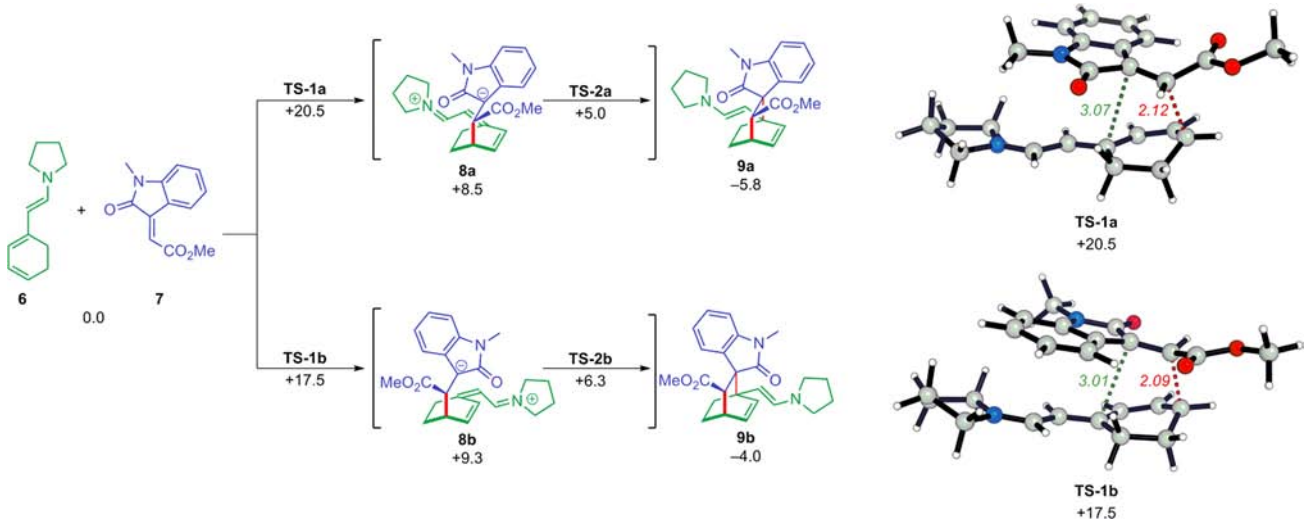

Scheme 3. Reaction Pathways for Cycloadditions of the Cross-Conjugated Trienamines 10 with the Oxindole 7 [Free Energies with Respect to 6 + 7, in kcal mol^{-1}; M06-2X/def2-TZVPP/IEFPCM//B97D/6-31+G(d,p)/IEFPCM]

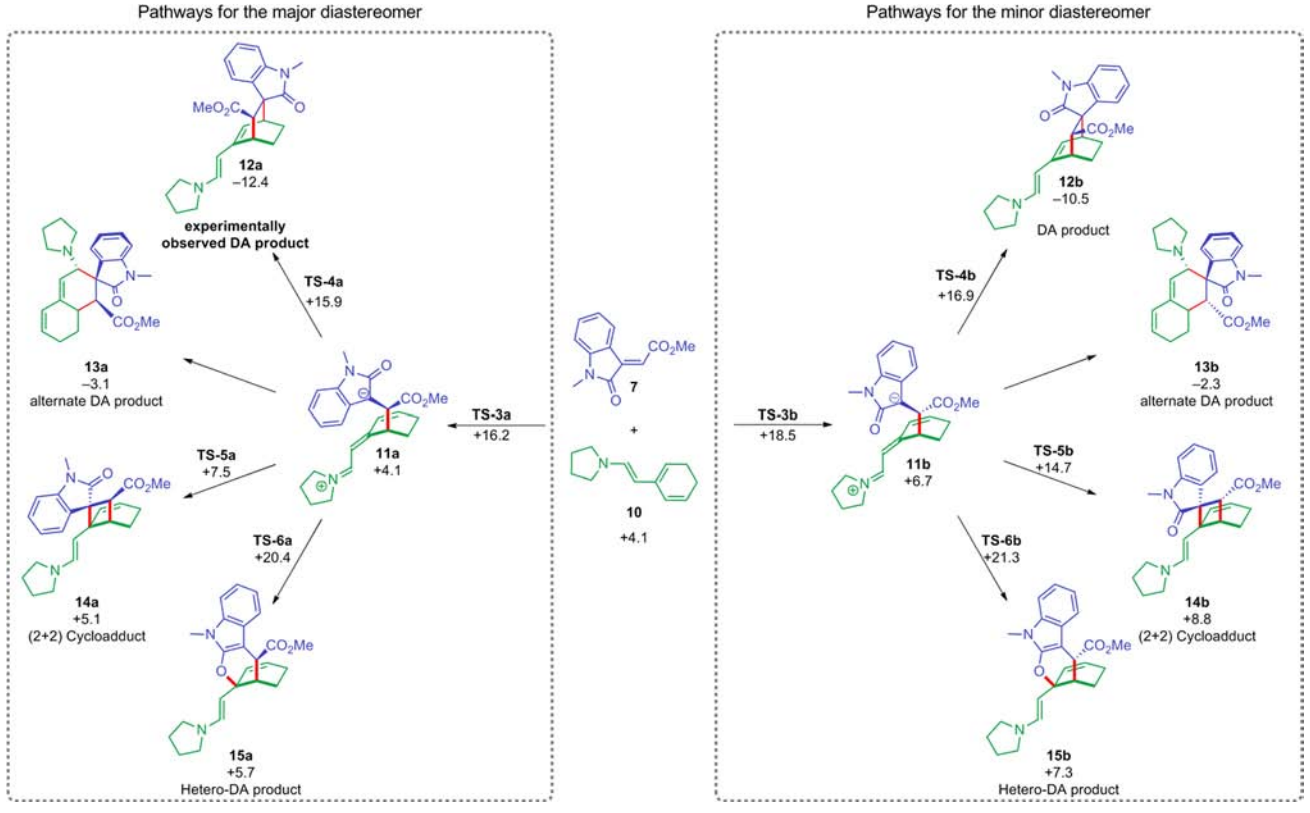

model system that has previously been used by Jørgensen (Schemes 2 and 3).[6] Furthermore, we explored the stereochemistry with the full diphenylsiloxy system. A rich variety of competing reactions has been uncovered, and a complex interplay of kinetics and thermodynamics dictates the ultimately very selective reaction.

■ COMPUTATIONAL METHODS

All structures were optimized employing B97D[7] and the double-ζ split-valence 6-31+G(d,p) basis set. Solvation by chloroform was taken into account using the integral equation formalism polarizable continuum model (IEFPCM)[8] in both optimizations and calculations of harmonic vibrational frequencies. It has recently been shown that the presence of a polarizable continuum model does not have a big impact on frequencies, while solvation is sometimes necessary to locate certain transition states that only exist in polar media.[9] Vibrational analysis verified that each structure was a minimum or a transition state. Thermal corrections were calculated from unscaled frequencies for a standard state of 298.15 K and 1 atm. Entropic contributions to the reported free energies were calculated from partition functions evaluated using Truhlar's quasiharmonic approximation.[9] This method uses the same approximations as the usual harmonic oscillator except that all vibrational frequencies lower than 100 cm^{-1} are set equal to 100 cm^{-1} to correct for

dx.doi.org/10.1021/ja312043g | J. Am. Chem. Soc. 2013, 135, 3237−3242

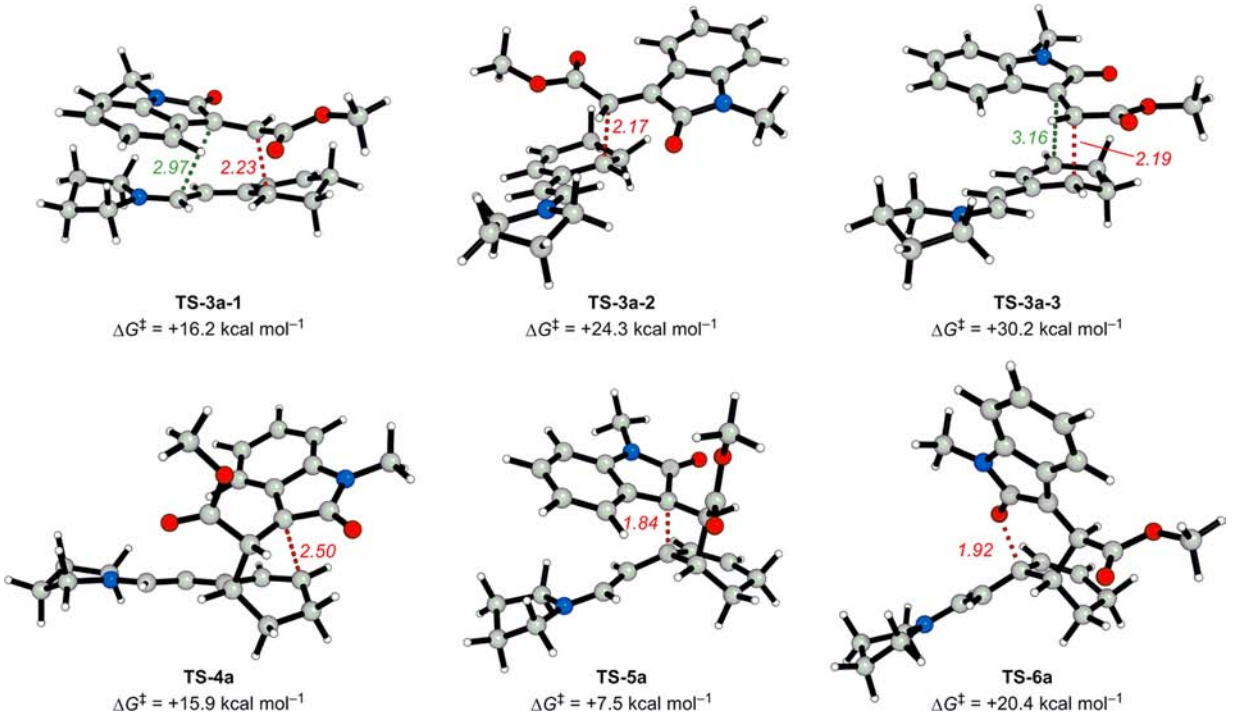

Figure 1. Transition state geometries and activation free energies (relative to **6** + **7**) for different conformers of **TS-3a** and for cyclizations leading to a Diels–Alder product (**TS-4a**), a (2 + 2) cycloadduct (**TS-5a**), and a hetero-Diels–Alder product (**TS-6a**) [M06-2X/def2-TZVPP/IEFPCM//B97D/6-31+G(d,p)/IEFPCM].

the breakdown of the harmonic oscillator approximation for low frequencies. Electronic energies were obtained from single-point calculations on the B97D geometries employing the M06-2X functional,[10] the large triple-ζ def2-TZVPP basis set, and IEFPCM for chloroform, a level expected to give accurate energies.[11] An ultrafine grid was used throughout this study for numerical integration of the density.[12] All computations were performed using Gaussian 09.[13]

RESULTS AND DISCUSSION

Linear Trienamine Reactivity. The cycloaddition reactions of the linear trienamine **6** with the oxindole **7** proceed via transition states **TS-1a** and **TS-1b** ($\Delta G^{\ddagger}$ = +20.5 and +17.5 kcal mol^{-1}, Scheme 2) to yield the zwitterionic intermediates **8a** and **8b**. In the transition states, the forming bonds are 2.12 and 2.09 Å, respectively, while the second pairs of carbon centers are well separated (~3 Å, Scheme 2). Transition states with different conformations (rotation around the forming C–C bond) were at least 6 kcal mol^{-1} higher in energy (see the Supporting Information for structures).

In contrast to gas-phase calculations by Jørgensen and coworkers,[6] our calculations employing a polarizable continuum model predict the zwitterions **8a** and **8b** to be shallow local minima on the B97D potential energy surfaces (PES). These results underline the need to account for solvation when dealing with highly polar structures. However, the barriers for the subsequent cyclization yielding **9a** and **9b** are very small. B97D calculations reveal very small activation energies ($\Delta G^{\ddagger}$ < 4 kcal mol^{-1}, relative to **8**), while negative barriers are obtained from M06-2X single-point calculation on the B97D-optimized structures. Thus, both methods predict **9a** and **9b** to be formed rapidly from **8a** and **8b**. This type of stepwise reactions involving ions or zwitterions and no significant barriers to closure of the second bond has been found previously.[14]

Cross-Conjugated Trienamine Reactivity. In line with Jørgensen's computational results,[6] the cross-conjugated trienamine **10** is thermodynamically less stable than its linear isomer **6** (ΔG = +4.1 kcal mol^{-1}, Scheme 3). The cross-conjugated species **10** reacts with oxindole **7** to form zwitterionic intermediates **11a** and **11b** via transition states **TS-3a** and **TS-3b** ($\Delta G^{\ddagger}$ = +16.2 and +18.5 kcal mol^{-1}, Scheme 3). The energetics of these reactions are shown in Schemes 3 and 4, and computed structures of various species involved are depicted in Figures 1 and 2. Conformer **TS-3a-1** possesses the lowest energy of all **TS3a** geometries (Figure 1) and adopts a geometry resembling alternate Diels–Alder adduct **13a**. The forming bond is about 0.1 Å longer than the corresponding bonds in **TS1** (Scheme 2). Rotation of the oxindole around the forming C–C bond affords conformer **TS-3a-2**, which is 8.1 kcal mol^{-1} higher in energy (Figure 1). Conformer **TS-3a-3** corresponds to the transition state reported by Jørgensen[6] and resembles Diels–Alder product **12a**. It is 14 kcal mol^{-1} higher in energy than **TS-3a-1** and, as a consequence, is not important for this transformation. Analogous transition state conformers for **TS-3b** are provided in the Supporting Information. Following the intrinsic reaction coordinate (IRC) starting from **TS-3a** and **TS-3b** and subsequent optimizations confirmed **11a** and **11b** as stationary points and zwitterionic intermediates. Attempts to locate a concerted mechanism starting from different transition state guesses failed. Therefore, these reactions are initiated by the attack of dienamines on Michael acceptors. The calculated energy difference between **TS-3a** and **TS-3b** is in good agreement with the preferred formation of the analogue of **12a** over its diastereomer **12b** (dr 8:1).[6]

In principle, the collapse of all zwitterionic intermediates **8** and **11** with formation of a variety of cycloadducts is possible (Scheme 3). The fate of all zwitterionic intermediates is provided in the Supporting Information, and only pathways involving **11a** will be discussed here as this intermediate leads to the product corresponding to the experimentally observed compounds (Schemes 3 and 4). Furthermore, as shown in Scheme 3, the activation energies for formation of **11b** and conversion to **12b–15b** are all unfavorable as compared to **12a–15a**.

dx.doi.org/10.1021/ja312043g | J. Am. Chem. Soc. 2013, 135, 3237–3242

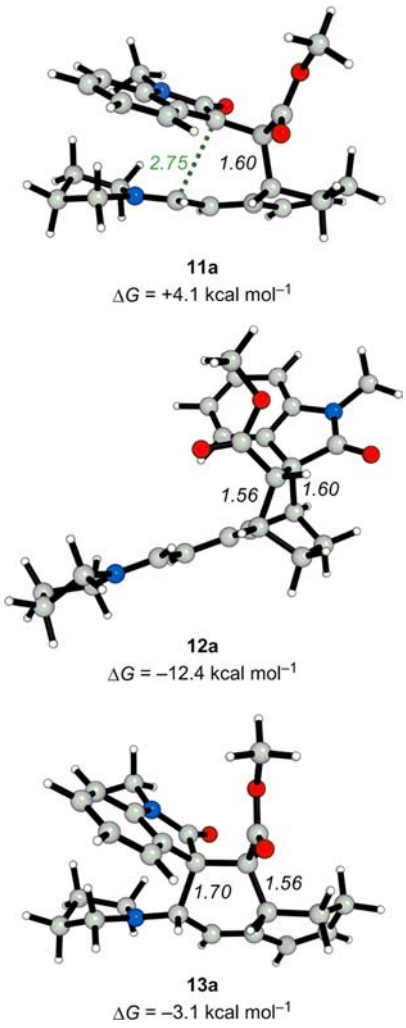

Figure 2. Calculated structures for the zwitterionic intermediate **11a**, Diels–Alder product **12a** corresponding to the experimentally observed product, and the alternate Diels–Alder product **13a** [M06-2X/def2-TZVPP/IEFPCM//B97D/6-31+G(d,p)/IEFPCM].

Zwitterion **11a** collapses to the alternate Diels–Alder product **13a** without a significant barrier. B97D calculations predict an activation energy of 5.2 kcal mol^{-1} (relative to **11a**), while a negative barrier is obtained from M06-2X single-point calculation on the B97D-optimized structure. Thus, this reaction occurs much faster than the initial C–C bond formation through **TS-3a**. This reaction is exergonic (ΔG = −3.1 kcal mol^{-1}) and yields **13a** (Figure 2). Due to the small exergonicity and the absence of a significant barrier, this reaction is reversible, which is also reflected in the elongated C–C bond. The long C–C bond correlates well with the reversibility of this reaction.

The collapse of zwitterionic intermediates in organocatalytic reactions to cyclobutanes is experimentally well-known, and these structures have been characterized by NMR spectroscopy.[4n,15] We also find a reaction leading to formal (2 + 2) adduct **14a**. This cycloaddition takes place via transition state **TS-5a** ($\Delta G^{\ddagger}$ = +7.5 kcal mol^{-1}, Schemes 3 and 4). The forming C–C bond in **TS5a** is quite short (1.84 Å, Figure 1) which correlates well with this reaction being endergonic by 1 kcal mol^{-1}. Therefore, if cyclobutane **14a** is formed at all, it readily reverses to zwitterion **11a**. In contrast to prior reports on organocatalytic Michael additions to nitroolefins,[4n,15] **14a** is not expected to be an experimentally observable intermediate.

Scheme 4. Free Energy Profile (relative to 6 + 7, in kcal mol^{-1}) for the Reactions of the Cross-Conjugated Trienamine 10 and the Oxindole 7 via TS-3a [M06-2X/def2-TZVPP/IEFPCM//B97D/6-31+G(d,p)/IEFPCM]

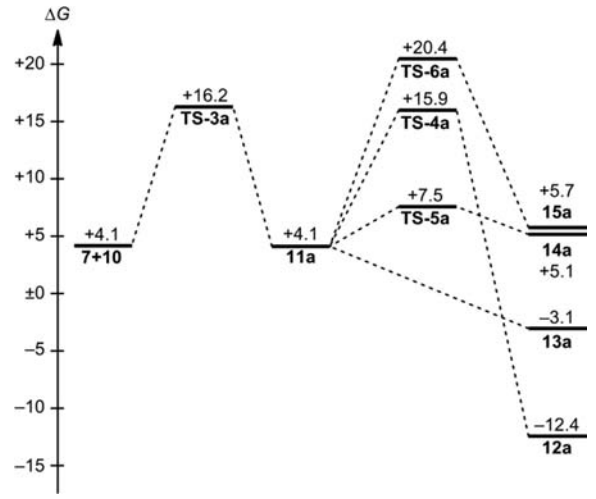

A nucleophilic attack of the enolate oxygen atom on the β-position of an unsaturated iminium ion **11a** is also conceivable and leads to the hetero Diels–Alder product **15a**. This reaction is endergonic (ΔG = +5.7 kcal mol^{-1}) and would have to proceed through the highest transition state **TS-6a** ($\Delta G^{\ddagger}$ = +20.4 kcal mol^{-1}, Figure 1). As a consequence, this transformation is unlikely to occur under the reaction conditions.

The formation of the Diels–Alder adduct **12a**, which corresponds to the experimentally observed product, proceeds via **TS-4a** ($\Delta G^{\ddagger}$ = +15.9 kcal mol^{-1}, Schemes 3 and 4). The forming C–C bond is 2.75 Å long, corresponding to a very early transition state (Figure 1). This reaction is strongly exergonic (ΔG = −12.4 kcal mol^{-1}) and leads to the thermodynamically most stable cycloadduct **12a**. The lengths of the two newly formed bonds are in good agreement (within 0.02–0.03 Å) with those derived from crystal structures of analogous cycloadducts synthesized by the Jørgensen group.[6]

Origin of Regioselectivity. The initial attack via **TS-3a** takes place with the smallest activation free energy and leads to the most stable zwitterionic intermediate. In line with this, transition state **TS-3a** has the smallest dipole moment of all **TS-1** and **TS-3** transition states. Intermediate **11a** is not only formed via the lowest barrier but is also the most stable zwitterionic intermediate. Both kinetic and thermodynamic control favors the formation of **11a** and thus determine the regio- and stereoselectivity of the initial bond formation. Although **TS-1b** is only 1.3 kcal mol^{-1} higher in energy and would be populated to some extent, the resulting products can revert to **6** and **7** to form the most stable product.

Starting from the preferentially formed intermediate **11a**, the (2 + 2) and hetero-Diels–Alder cycloadditions do not yield stable products (**14a** and **15a**) and readily revert to **11a**. The alternate Diels–Alder product **13a** is stable with respect to reactants, and analogous compounds used in experiments should be amenable to spectroscopic *in situ* characterization (e. g., NMR spectroscopy) at early stages of the reaction. However, the low barrier for the backward reaction allows its isomerization to the thermodynamically most stable cycloadduct **12a** via **TS-4a**. Thus, the regiochemistry of the second bond formation is thermodynamically controlled, as **12a** is not expected to revert to **11a** (Scheme 4).

dx.doi.org/10.1021/ja312043g | J. Am. Chem. Soc. 2013, 135, 3237–3242

Origin of Enantioselectivity. In their experiments, Jørgensen and co-workers observed excellent enantioselectivities (typically >97%) with diphenylprolinol-derived trienamines.[6] On the basis of insights obtained from the model system, we studied the enantioselectivity of the experimental chiral trienamine (Scheme 5). The transition state geometry for the sterically less hindered attack ***anti*-TS-7** resembles that of **TS-3a** in the model system and displays almost identical distances between the reaction centers. In line with previous experimental and theoretical investigations,[16] the *sc-exo* conformation for the OTMS group was found to be most stable. The corresponding attack from the hindered side proceeds via ***syn*-TS-7** with an electrostatically unfavorable alignment of **3** and **7**. This change in geometry can be attributed to the steric demand of the bulky substituent that prevents the favored alignment found in **TS-3a**. In the smaller model system (see Figure 1), this conformation is 8 kcal mol^{-1} higher in energy than the more favorable conformation found in **TS-3a** and ***anti*-TS-7**. Thus, the energy difference of 12.8 kcal mol^{-1} between ***syn*-TS-7** and ***anti*-TS-7** is mainly caused by the conformational change enforced by the diphenylsiloxy substituent. In analogy to the model system described above, ***anti*-TS-7** can lead to an alternate Diels–Alder product, which isomerizes to yield ***anti*-17** after hydrolysis. In summary, the high enantioselectivity of the overall reaction is a result of the large energetic difference between ***anti*-TS-7** and ***syn*-TS-7** (i.e., kinetic control) so that no ***syn*-17** will be formed even with the assumption of all reactions being reversible. Our computations are in agreement with the experimental observation of almost exclusive formation of ***anti*-17**.

Scheme 5. Transition State Geometries and Relative Activation Energies (in kcal mol^{-1}) for the Reaction of the Diarylprolinol Enamine 3 with the Oxindole 7 [M06-2X/def2-TZVPP/IEFPCM//B97D/6-31+G(d,p)/IEFPCM]

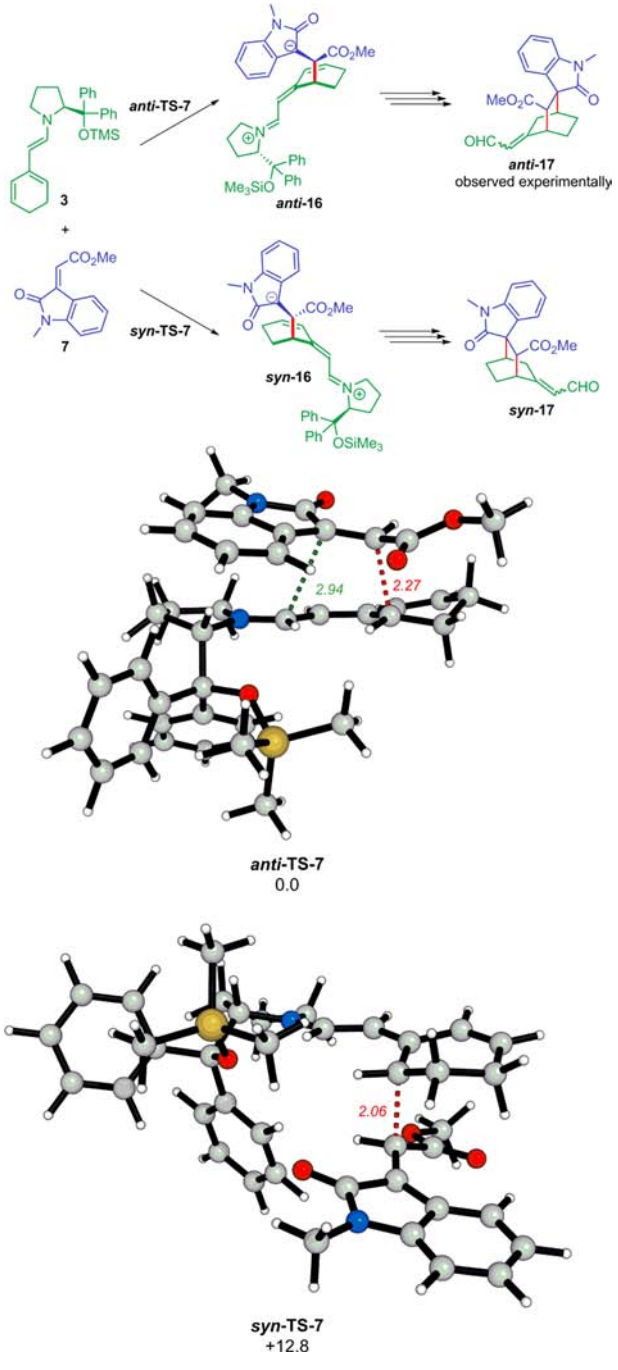

CONCLUSIONS

Our calculations show strong evidence for stepwise mechanisms and a variety of intermediates in [4 + 2] cycloaddition reactions of cyclic trienamines and oxindoles. The selectivities of these Diels–Alder reactions can be explained by kinetic and thermodynamic control of the formation of the zwitterionic intermediate **11a** and a thermodynamically controlled isomerization of the alternate cycloadduct **13a** to **12a**. The observed high enantioselectivity and pronounced energetic difference between diastereomeric transition states ***anti*-TS-7** and ***syn*-TS-7** are a consequence of conformational changes in transition states for the initial bond formation enforced by the diphenylsiloxy substituent. The roles of unobserved intermediates in such highly selective reactions provide a cautionary tale to the interpretation of selectivity involving such highly activated reactants.

ASSOCIATED CONTENT

Supporting Information

Cartesian coordinates and energies of all reported structures, details of computational methods, and complete ref 13. This material is available free of charge via the Internet at http://pubs.acs.org.

AUTHOR INFORMATION

Corresponding Author

houk@chem.ucla.edu

Author Contributions

‡A.D. and M.B. contributed equally.

Notes

The authors declare no competing financial interest.

ACKNOWLEDGMENTS

We are grateful to the Alexander von Humboldt Foundation (Feodor-Lynen scholarships to A.D. and M.B.) and the National Science Foundation (CHE-0548209 to K.N.H.) for financial support. This work used the Extreme Science and Engineering Discovery Environment (XSEDE), which is supported by National Science Foundation Grant Number OCI-1053575 and resources from the UCLA Institute for Digital Research and Education (IDRE).

REFERENCES

(1) (a) Berkessel, A.; Gröger, H. *Asymmetric Organocatalysis: From Biomimetic Concepts to Applications in Asymmetric Synthesis*; Wiley-VCH: Weinheim, 2005. (b) Dalko, P. I., Ed. *Enantioselective Organocatalysis*; Wiley-VCH: Weinheim, 2007. (c) Waser, M. *Asymmetric Organocatalysis in Natural Product Syntheses*; Springer: Heidelberg, 2012. (d) Erkkilä, A.; Majander, I.; Pihko, P. M. *Chem. Rev.* **2007**, *107*, 5416−5470. (e) Mukherjee, S.; Yang, J. W.; Hoffmann, S.; List, B. *Chem. Rev.* **2007**, *107*, 5471−5569. (f) Beeson, T. D.; Mastracchio, A.; Hong, J.-B.; Ashton, K.; MacMillan, D. W. C. *Science* **2007**, *316*, 582−585. (g) MacMillan, D. W. C. *Nature* **2008**, *455*, 304−308. (h) Melchiorre, P.; Marigo, M.; Carlone, A.; Bartoli, G. *Angew. Chem., Int. Ed.* **2008**, *47*, 6138−6171. (i) Ramachary, D. B.; Reddy, Y. V. *Eur. J. Org. Chem.* **2012**, *2012*, 865−887. (j) Jensen, K. L.; Dickmeiss, G.; Jiang, H.; Albrecht, Ł.; Jørgensen, K. A. *Acc. Chem. Res.* **2012**, *45*, 248−264.

(2) Li, J.-L.; Liu, T.-Y.; Chen, Y.-C. *Acc. Chem. Res.* **2012**, *45*, 1491−1500.

(3) Houk, K. N. *Acc. Chem. Res.* **1975**, *8*, 361−369.

(4) (a) Juhl, K.; Jørgensen, K. A. *Angew. Chem., Int. Ed.* **2003**, *42*, 1498−1501. (b) Ramachary, D. B.; Chowdari, N. S.; Barbas, C. F., III. *Angew. Chem., Int. Ed.* **2003**, *42*, 4233−4237. (c) Clark, R. C.; Pfeiffer, S. S.; Boger, D. L. *J. Am. Chem. Soc.* **2006**, *128*, 2587−2593. (d) He, M.; Struble, J. R.; Bode, J. W. *J. Am. Chem. Soc.* **2006**, *128*, 8418−8420. (e) Bertelsen, S.; Marigo, M.; Brandes, S.; Dinér, P.; Jørgensen, K. A. *J. Am. Chem. Soc.* **2006**, *128*, 12973−12980. (f) Han, B.; Li, J.-L.; Ma, C.; Zhang, S.-J.; Chen, Y.-C. *Angew. Chem., Int. Ed.* **2008**, *47*, 9971−9974. (g) de Figueiredo, R. M.; Fröhlich, R.; Christmann, M. *Angew. Chem., Int. Ed.* **2008**, *47*, 1450−1453. (h) Bencivenni, G.; Wu, L.-Y.; Mazzanti, A.; Giannichi, B.; Pesciaioli, F.; Song, M.-P.; Bartoli, G.; Melchiorre, P. *Angew. Chem., Int. Ed.* **2009**, *48*, 7200−7203. (i) Han, B.; He, Z.-Q.; Li, J.-L.; Li, R.; Jiang, K.; Liu, T.-Y.; Chen, Y.-C. *Angew. Chem., Int. Ed.* **2009**, *48*, 5474−5477. (j) Jia, Z.-J.; Jiang, H.; Li, J.-L.; Gschwend, B.; Li, Q.-Z.; Yin, X.; Grouleff, J.; Chen, Y.-C.; Jørgensen, K. A. *J. Am. Chem. Soc.* **2011**, *133*, 5053−5061. (k) Jiang, H.; Gschwend, B.; Albrecht, Ł.; Hansen, S. G.; Jørgensen, K. A. *Chem.—Eur. J.* **2011**, *17*, 9032−9036. (l) Jia, Z.-J.; Zhou, Q.; Zhou, Q.-Q.; Chen, P.-Q.; Chen, Y.-C. *Angew. Chem., Int. Ed.* **2011**, *50*, 8638−8641. (m) Liu, Y.; Nappi, M.; Arceo, E.; Vera, S.; Melchiorre, P. *J. Am. Chem. Soc.* **2011**, *133*, 15212−15218. (n) Albrecht, Ł.; Dickmeiss, G.; Cruz Acosta, F.; Rodríguez-Escrich, C.; Davis, R. L.; Jørgensen, K. A. *J. Am. Chem. Soc.* **2012**, *134*, 2543−2546. (o) Xiong, X.-F.; Zhou, Q.; Gu, J.; Dong, L.; Liu, T.-Y.; Chen, Y.-C. *Angew. Chem., Int. Ed.* **2012**, *51*, 4401−4404. (p) Arceo, E.; Melchiorre, P. *Angew. Chem., Int. Ed.* **2012**, *51*, 5290−5292.

(5) (a) Albrecht, Ł.; Cruz Acosta, F.; Fraile, A.; Albrecht, A.; Christensen, J.; Jørgensen, K. A. *Angew. Chem., Int. Ed.* **2012**, *51*, 9088−9092. (b) Jiang, H.; Rodríguez-Escrich, C.; Johansen, T. K.; Davis, R. L.; Jørgensen, K. A. *Angew. Chem., Int. Ed.* **2012**, *51*, 10271−10274.

(6) Halskov, K. S.; Johansen, T. K.; Davis, R. L.; Steurer, M.; Jensen, F.; Jørgensen, K. A. *J. Am. Chem. Soc.* **2012**, *134*, 12943−12946.

(7) Grimme, S. *J. Comput. Chem.* **2006**, *27*, 1787−1799.

(8) Cancès, E.; Mennucci, B.; Tomasi, J. *J. Chem. Phys.* **1997**, *107*, 3032−3041.

(9) Ribeiro, R. F.; Marenich, A. V.; Cramer, C. J.; Truhlar, D. G. *J. Phys. Chem. B* **2011**, *115*, 14556−14562.

(10) Zhao, Y.; Truhlar, D. *Theor. Chem. Acc.* **2008**, *120*, 215−241.

(11) Goerigk, L.; Grimme, S. *Phys. Chem. Chem. Phys.* **2011**, *13*, 6670−6688.

(12) Wheeler, S. E.; Houk, K. N. *J. Chem. Theory Comput.* **2010**, *6*, 395−404.

(13) Frisch, M. J.; et al. *Gaussian 09*, Revision C.01; Gaussian, Inc.: Wallingford CT, 2009.

(14) Iafe, R. G.; Houk, K. N. *J. Org. Chem.* **2008**, *73*, 2679−2686.

(15) (a) Patora-Komisarska, K.; Benohoud, M.; Ishikawa, H.; Seebach, D.; Hayashi, Y. *Helv. Chim. Acta* **2011**, *94*, 719−745. (b) Burés, J.; Armstrong, A.; Blackmond, D. G. *J. Am. Chem. Soc.* **2011**, *133*, 8822−8825. (c) Burés, J.; Armstrong, A.; Blackmond, D. G. *J. Am. Chem. Soc.* **2012**, *134*, 6741−6750. (d) Parra, A.; Reboredo, S.; Alemán, J. *Angew. Chem., Int. Ed.* **2012**, *51*, 9734−9736.

(16) Grošelj, U.; Seebach, D.; Badine, D. M.; Schweizer, W. B.; Beck, A. K.; Krossing, I.; Klose, P.; Hayashi, Y.; Uchimaru, T. *Helv. Chim. Acta* **2009**, *92*, 1225−1259. (b) Schmid, M. B.; Zeitler, K.; Gschwind, R. M. *Chem. Sci.* **2011**, *2*, 1793−1803.